

Accepted Manuscript

Synthesis, biological evaluation and molecular modeling of a novel series of fused 1,2,3-triazoles as potential anti-coronavirus agents

Konstantina Karypidou, Sergio R. Ribone, Mario A. Quevedo, Leentje Persoons, Christophe Pannecouque, Christine Helsen, Frank Claessens, Wim Dehaen

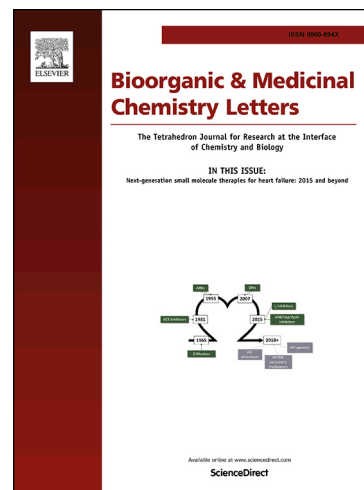
PII: S0960-894X(18)30750-9
DOI: <https://doi.org/10.1016/j.bmcl.2018.09.019>
Reference: BMCL 26040

To appear in: *Bioorganic & Medicinal Chemistry Letters*

Received Date: 25 July 2018
Revised Date: 11 September 2018
Accepted Date: 15 September 2018

Please cite this article as: Karypidou, K., Ribone, S.R., Quevedo, M.A., Persoons, L., Pannecouque, C., Helsen, C., Claessens, F., Dehaen, W., Synthesis, biological evaluation and molecular modeling of a novel series of fused 1,2,3-triazoles as potential anti-coronavirus agents, *Bioorganic & Medicinal Chemistry Letters* (2018), doi: <https://doi.org/10.1016/j.bmcl.2018.09.019>

This is a PDF file of an unedited manuscript that has been accepted for publication. As a service to our customers we are providing this early version of the manuscript. The manuscript will undergo copyediting, typesetting, and review of the resulting proof before it is published in its final form. Please note that during the production process errors may be discovered which could affect the content, and all legal disclaimers that apply to the journal pertain.



Synthesis, biological evaluation and molecular modeling of a novel series of fused 1,2,3-triazoles as potential anti-coronavirus agents

Konstantina Karypidou^a, Sergio R. Ribone^b, Mario A. Quevedo^b, Leentje Persoons^c, Christophe Pannecouque^c,
Christine Helsen^d, Frank Claessens^d and Wim Dehaen^{a*}

^a Molecular Design and Synthesis, Department of Chemistry, KU Leuven, Celestijnenlaan 200F, 3001, Leuven, Belgium

*wim.dehaen@kuleuven.be, konstantina.karypidou@kuleuven.be,

^b Unidad de Investigación y Desarrollo en Tecnología Farmacéutica (UNITEFA, CONICET), Dpto. Farmacia, Fac. Ciencias Químicas, Universidad Nacional de Córdoba, Córdoba, X5000HUA, Argentina
alfredoq@fcq.unc.edu.ar, sribone@fcq.unc.edu.ar

^c Department of Microbiology and Immunology, Laboratory of Virology and Chemotherapy, Rega Institute for Medical Research, KU Leuven, Herestraat 49, B-3000 Leuven, Belgium
christophe.pannecouque@kuleuven.be, leentje.persoons@kuleuven.be

^d Laboratory of Molecular Endocrinology, Department of Cellular and Molecular Medicine, KU Leuven, Herestraat 49, B-3000 Leuven, Belgium
frank.claessens@kuleuven.be, christine.helsen@kuleuven.be

Abstract

Synthesis and biological evaluation of a novel library of fused 1,2,3-triazole derivatives are described. **The in-house developed** multicomponent reaction based on commercially available starting materials was applied and broad biological screening against various viruses was performed, showing promising antiviral properties for compounds **14d**, **14n**, **14q**, **18f** and **18i** against human coronavirus 229E. Further *in silico* studies identified the key molecular interactions between those compounds and the 3-chymotrypsin-like protease, which is essential to the intracellular replication of the virus, supporting the hypothesis that the protease is the target molecule of the potential antiviral derivatives.

Keywords: Respiratory Syndrome, Coronavirus, 3CL protease, 1,2,3-triazole, biological evaluation

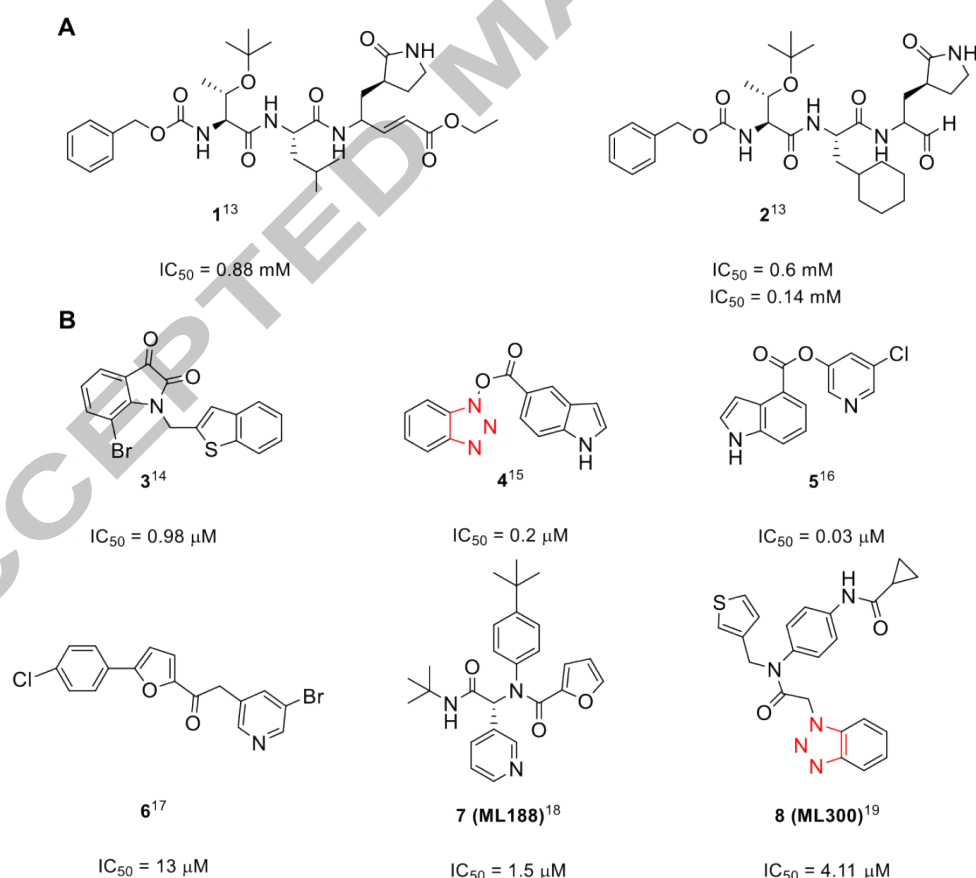
Coronaviruses are single-stranded RNA viruses associated with mild to severe respiratory symptoms. Human coronaviruses (HCoV) strains HCoV-229E and HCoV-OC43 were first described in the 1960s as causes for respiratory tract infections in humans, including common cold and pneumonia.¹ In 2002-2003, a new human coronavirus, named SARS-CoV, was identified as the etiological agent for the global outbreak of severe acute respiratory syndrome (SARS), which caused the death of over 800 individuals among 8000 cases worldwide, representing a fatality rate of almost 10%.^{2,3,4} Since then three additional coronaviruses have been recognized. Initially, HCoV-NL63⁵ and HCoV-HKU1,⁶ were reported causing acute respiratory diseases of lower severity compared to the SARS-CoV and more recently, Middle East respiratory syndrome (MERS-CoV) causing lethal respiratory diseases.^{7,8} To date, there are no approved antiviral drugs or vaccines available for the prevention and/or treatment of SARS-like viruses making the development of effective antiviral agents an imperative need.⁹

Coronaviruses express two proteases, a papain-like protease (PL^{pro}) and a 3-chymotrypsin-like protease (3CL^{pro}). The 3CL^{pro} enzyme, also referred to as Main protease (M^{pro}), is essential to the intracellular viral replication, making it an attractive target for the development of novel inhibitors.¹⁰ Reports in the literature

1 classify potential antiviral compounds into two main categories: i) the peptidomimetics (Fig. 1A) and ii) small
 2 molecule-based inhibitors (Fig. 1B) presenting both activities in μM and nM range. Despite the satisfying initial
 3 results, the majority of those promising compounds did not proceed to clinical studies due to nonideal
 4 physicochemical properties.⁹

5 References on non-peptidic inhibitors accentuate the presence of the benzotriazole group. The
 6 importance of this benzotriazole motif relies on the formation of key interactions with the catalytic dyad,
 7 Cys145 and His41, of the 3CL^{pro} active site.¹¹ Considering our interest in the chemistry of 1,2,3-triazole
 8 bioactive molecules and their interesting binding mode, we wanted to prepare a novel library of fused 1,2,3-
 9 triazoles and subsequently determine their biological activity.

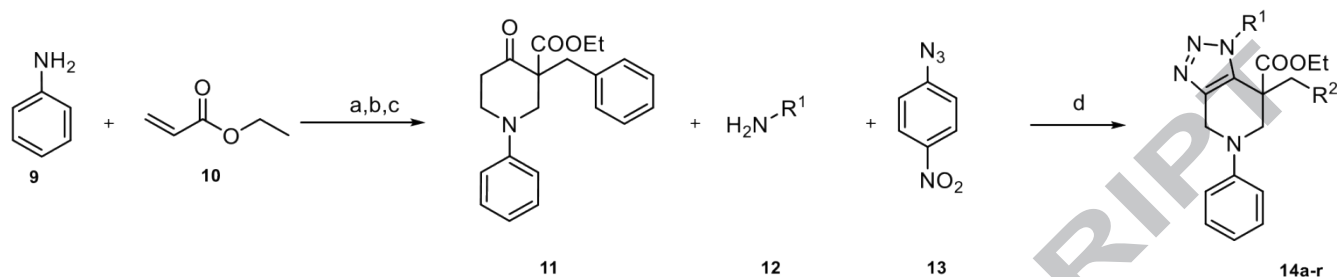
10 Here, we reported our preliminary results on the development of a novel series of fused 1,2,3-triazole
 11 compounds and their potential antiviral activity. For this purpose, we implemented the multicomponent
 12 reaction developed within our group, which resulted in a plethora of 1,2,3-triazole derivatives in a single step
 13 starting from readily available enolizable carbonyl compounds, primary amines and 4-nitrophenyl azide. In
 14 general, the method proceeds *via* an equilibrium of imine/enamine followed by [3+2] cycloaddition with the
 15 azide.¹² This leads to a triazolone intermediate which after elimination of 4-nitroaniline results in the final fused
 16 1,2,3-triazole analogues.



18 **Figure 1.** Representative A) peptidic¹³ and B) small molecule SARS-CoV 3CL^{pro} inhibitors¹⁴⁻¹⁹

20 The synthesis, presented in Scheme 1, began by following a general method to generate the
 21 oxopiperidine carboxylate intermediate which involves Michael addition of aniline onto ethyl acrylate followed

1 by an intramolecular Dieckmann condensation.²⁰ Subsequent nucleophilic substitution with benzyl bromide
 2 provided the starting material **11** in 65% overall yield. Once **11** was obtained, we proceeded for the fused
 3 triazole formation using a collection of primary amines and 4-nitrophenyl azide (PNA, **13**).



4

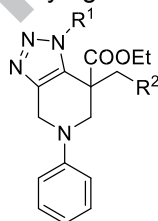
5 **Scheme 1.** Synthetic pathway towards derivatives **14a-r**. Reagents and conditions: (a) AcOH, CuCl, 24h, 110
 6 °C, 55%, (b) NaH, Toluene, EtOH, 6h, 100 °C, 90%, (c) BnBr, K₂CO₃, THF, 6h, 70 °C, 65%, (d) Toluene, 18h,
 7 100 °C.

8

9 We commenced our investigations with benzylic amines bearing both electron-donating functional
 10 groups, (Table 1, **14b-c**) and electron-withdrawing groups, (Table 1, **14d-j**). Both families were obtained in
 11 moderate to good yields.

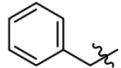
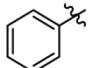
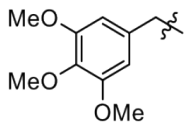
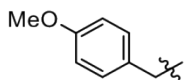
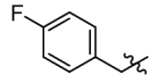
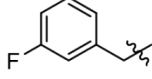
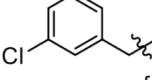
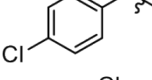
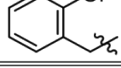
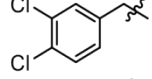
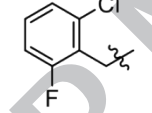
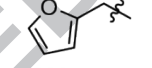
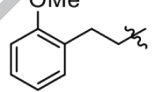
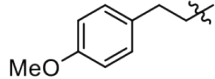
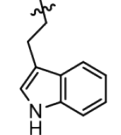
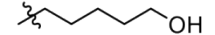

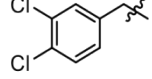
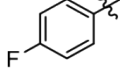
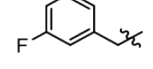
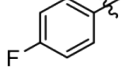
12

13 **Table 1.** Molecular structures, yield and biological activity against coronavirus (229E) of derivatives **14a-r**.



14

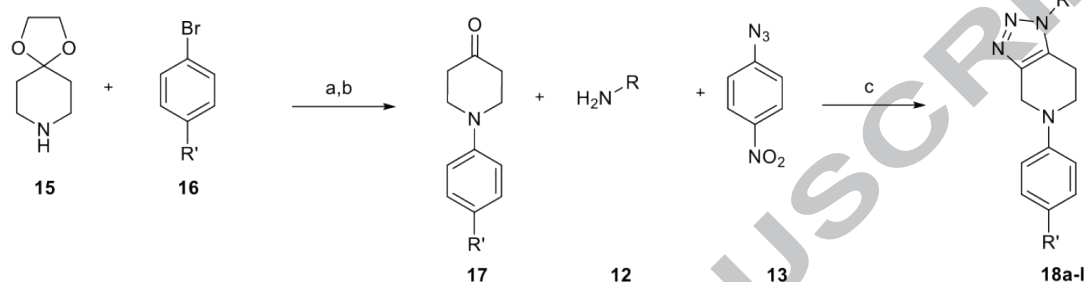
Entry	Compound ID	R ¹	R ²	Yield	EC ₅₀ (μM) ^a
-------	-------------	----------------	----------------	-------	------------------------------------

1	14a			80%	>100
2	14b			85%	>100
3	14c			65%	>100
4	14d			80%	8.95
5	14e			58%	>100
6	14f			80%	>100
7	14g			67%	>100
8	14h			48%	>100
9	14i			30%	>100
10	14j			73%	>100
11	14k			55%	>100
12	14l			56%	>100
13	14m			85%	>100
14	14n			80%	9.45
15	14o			57%	>100
16	14p			51%	>100
17	14q			50%	9.45
18	14r			60%	>100

^aConcentration required to reduce virus-induced cytopathogenicity by 50%

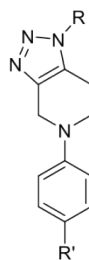
Further analysis using heterocyclic and aliphatic derivatives **14k-p** proved the applicability of these substituents under the high temperature conditions used in this reaction (Table 1). Furthermore, we examined the influence of the introduction of a fluoro group on the benzyl bromide on the reactivity (Table 1, entries **7** and **8**), which demonstrated that there is no effect on the outcome of the reaction.

1 A second series of fused 1,2,3-triazole analogues was prepared based on the previously described
 2 multicomponent method, starting from *N*-phenyl-4-piperidone material **17** which in turn was synthesized
 3 according to Buchwald-Hartwig Pd-catalyzed amination of different aryl bromides, presented in Scheme 2.²¹
 4 We initially examined the scope of this reaction with respect to primary amines. As we would expect based on
 5 the aforementioned results, we managed to synthesize an adequate number of examples in good to excellent
 6 yields (**18a-d**). Furthermore, the presence of electron withdrawing substituents on the aryl bromides was
 7 explored (**18e-l**). The results are summarized in Table 2.



9 **Scheme 2.** Reagents and conditions: (a) Pd(OAc)₂, XPhos, NaO-*t*-Bu, Toluene / *t*-BuOH (5:1), 18 h, 120 °C ,
 10 65%, (b) aq. HCl (5N), 3 h, 100 °C, 45%,(c) Toluene, 18 h, 100 °C.

11 **Table 2.** Molecular structures, yield and biological activity against coronavirus (229E) of derivatives **18a-l**.



Entry	Compound ID	R	R'	Yield	EC ₅₀ (μM) ^a
1	18a		H	85%	>100
2	18b			74%	>100
3	18c			90%	>100
4	18d			48%	>100
5	18e		-CF ₃	90%	>100
6	18f			85%	8.9
7	18g			85%	>100
8	18h			89%	>100
9	18i			85%	11.95
10	18j			89%	>100
11	18k		-F	91%	>100
12	18l			57%	>100

^aConcentration required to reduce virus-induced cytopathogenicity by 50%.

The compounds were evaluated against a broad variety of viruses including HIV-1 (strain III_B), HIV-2 (strain ROD) in MT-4 cells, herpes simplex virus type 1 (strain KOS), herpes simplex virus type 2 (strain G), herpes simplex virus type 1 TK⁻ (KOS) ACV^{res}, vaccinia virus, adeno virus-2 and coronavirus (229E) in HEL cells and their inhibitory activity was compared to that of reference compounds as zidovudine, brivudine, cidofovir, acyclovir, ganciclovir, zalcitabine, alovudine and *Urtica dioica* agglutinin (UDA), respectively. All compounds were inactive towards all tested viruses, while **14d** (EC₅₀ = 8.95 μM), **14n** (EC₅₀ = 9.45 μM), **14q** (EC₅₀ = 9.45 μM), **18f** (EC₅₀ = 8.90 μM) and **18i** (EC₅₀ = 11.95 μM) showed moderate activity against human coronavirus (229E), but all approximately 50 fold lower than the activity observed with UDA (EC₅₀ = 0.2 μM). No alterations of the normal cell morphology in confluent HEL cell

1 cultures was observed at concentrations up to 100 μM (data not shown). The selectivity index (SI)
2 (MCC/EC₅₀ ratio) was greater than 8 for all active compounds.

3 To determine the structure-activity relationship (SAR) for the synthesized library of fused 1,2,3-
4 triazoles, it is of utmost importance to identify the key intermolecular contacts involved in the non-covalent
5 interaction between 3CL^{pro} and the structurally diverse inhibitors. With this aim, several molecular modeling
6 techniques, including molecular docking, molecular dynamics, free energy of binding analyses and
7 intermolecular interaction scanning, were applied in the search of such SAR knowledge. In a first stage,
8 previously reported 3CL^{pro} non-covalent inhibitors were modeled in order to define the key intermolecular
9 interactions required for enzyme inhibition, while in a second stage the *in silico* analysis was extended to
10 the family of fused 1,2,3-triazoles presented in this report.

11 The catalytic activity of 3CL^{pro} has been well characterized, with extensive details regarding the
12 structure of this enzyme and the corresponding catalytic site. In this respect, it is known that the active site
13 is located within domains I and II, in which a catalytic dyad consisting of residues Cys145 and His41 is
14 located.¹¹ It has also been previously reported that the catalytic site of 3CL^{pro} exhibits a stereoselective
15 recognition of non-covalent inhibitors.¹⁸ In this context, our molecular modeling protocols initiated with the
16 exploration of the binding mode, intermolecular interaction pattern and stereoselectivity of the non-covalent
17 inhibitor of 3CL^{pro} deposited in the Protein Databank under the code 3V3M. Both enantiomers of the bound
18 ligand were docked within the catalytic site, and as can be seen in Fig S1.a,b, the *R* enantiomer resulted in
19 an identical interaction pattern to that observed in the experimentally obtained crystal. The ligand binding is
20 stabilized by several hydrophobic and hydrogen bond (HB) interaction, of which those with Glu166, His163
21 and Gly143 are of particular relevance. Noteworthy, the *S* enantiomer was also able to establish several
22 hydrophobic interactions, but was not able to establish HB with Glu166 and His163. Taking into account
23 that it has been previously reported that only the *R* enantiomer is active,¹⁸ this finding suggests that the
24 establishment of interactions with Glu166 and His163 constitutes a critical feature to inhibit the catalytic
25 activity of the enzyme. To further study the persistence of these HB interactions, the intermolecular
26 complexes were subjected to molecular dynamics (MD) analysis, with Table S1 presenting the persistence
27 value (%) for each HB as calculated from the MD trajectories. As can be seen in Table S1, entry 1, the *R*
28 enantiomer was able to maintain in relatively high frequencies the HB interactions with Glu166, His163 and
29 Gly143, while the *S* enantiomer rearranged its binding to contact only Glu166 (60 % persistence). Our
30 findings not only validate the molecular modeling workflow we developed (i.e. the crystallographic binding
31 pose was reproduced), but also strongly suggests that at least two stable electrostatic interactions within
32 the active site are required for effective 3CL^{pro} inhibition.

33 To further study this hypothesis, a set of 12 previously reported 3CL^{pro} inhibitors containing a fused
34 1,2,3 triazole ring and exhibiting a wide range of inhibitory activities (i.e. between 51-26000 nM, Tables
35 S3S5), was subjected to our molecular modeling workflow. The lowest energy binding mode obtained for
36 TS8 was in agreement with the reported crystallographic structure (Fig. S3.d and pdb code 4MDS,
37 respectively), further supporting an adequate parametrization and simulation conditions of the molecular
38 modeling protocol. From inspection of the corresponding lowest energy docked poses for the whole set of
39 compounds (Figures S2-S4), we observed that all these inhibitors were indeed able to establish the two
40 HB previously described for 3V3M, i.e. one with the backbone of Glu166 and another one with the side

1 chain of His163. In these binding modes, the triazole ring is positioned in the proximity of the catalytic
2 dyad. From the MD simulations and the quantification of the persistence of the above mentioned hydrogen
3 bond interactions (Table S1, entries **3-14**), we observed that all the compounds maintained the hydrogen
4 bonds required for the inhibition of 3CL^{pro} in high frequencies, and in particular that with Glu166. It is
5 noteworthy that inhibitors that are enantiomerically pure and exhibiting submicromolar activities maintained
6 high frequencies of HB with Glu166 and His163. In particular, TS-1, which is by far the most potent
7 compound within the training set, exhibited also a single cluster of docked poses, suggesting not only an
8 efficient pharmacodynamic interaction with 3CL^{pro}, but also an adequate conformational preorganization
9 that is compliant with the corresponding bioactive conformation.

10 Compounds **14a-r** and **18a-l** were subjected to the molecular modeling workflows in order to study
11 whether 3CL^{pro} may represent a plausible molecular target for their observed antiviral activity. Figures
12 S5S9 shows the lowest energy binding modes to 3CL^{pro} found for compounds **14a-r**. When the docked
13 poses corresponding to the bioactive derivatives are observed (*i.e.* **14d** and **14n**, Figures S5.d, S8.b,
14 respectively), it can be seen that they establish the two HB interactions with Glu166 and His163,
15 positioning also the triazole ring in the proximities of the catalytic dyad. As it was discussed in previous
16 sections, this interaction pattern is required for the inhibition of 3CL^{pro} catalytic activity, suggesting that this
17 enzyme may be the antiviral target of these fused 1,2,3-triazoles. Further analysis by MD also showed that
18 these interactions are maintained throughout the simulation, further supporting their bioactivities (Table S2,
19 entries 4, 14 and 17). In contrast, the fused triazole derivatives that did not exhibited antiviral activities in
20 infected cells, did not establish these two HB interactions in the lowest energy binding pose, or were not
21 able to form them during the simulation trajectory when subjected to MD assays. Compounds **14c** and
22 **14m** constitute two exceptions to this behavior, both of them bearing a methoxy substituent on the para
23 position of the phenyl ring substituting the triazole central scaffold. These two compounds were able to
24 establish and maintain the HB interaction pattern required for 3CL^{pro} inhibition, (Table S2, entries 3 and 13)
25 but did not exhibit antiviral activity. This fact may be due to a disfavorable entropic contribution upon
26 binding to the 3CL^{pro} catalytic site, since in order to maintain the interaction with His163, the rotation of the
27 methoxy group is constrained within a dihedral angle of 10 Å. Clearly, this entropic cost is not present for
28 the bioactive analogue bearing a fluorine atom in the para position (**14d**).

29 When derivatives **18a-l** were analyzed (Figures S10-S12), a similar behavior was observed, with the
30 derivatives exhibiting antiviral activity (*i.e.* **18f** and **18i**) being able to establish two stable HB interactions
31 within the catalytic site of 3CL^{pro} (Figures S11.b and S12.a). In particular, derivative **18f** is anchored within
32 the catalytic site through a stable interaction with His163, with two additional interactions being established
33 with Glu166 and Thr25. Regarding the interaction of **18i**, this compound establishes stable HB contacts
34 with both Glu166 and His163, while further anchoring to residue Gln189. As a result, both compounds
35 positioned the fused triazole scaffold in the vicinity of the catalytic dyad which is consistent with blocking
36 the protease activity of the enzyme. Finally, when the interaction patterns of the inactive compounds within
37 the series **18a-l** were analyzed, we found that all of them failed to establish the two required HB
38 interactions within the catalytic site of the enzyme.

39 In conclusion, we have succeeded in synthesizing a novel library of fused 1,2,3-triazoles using the in-
40 house developed multicomponent reaction. The library was subjected to *in vitro* analysis using a broad

1 variety of viruses to determine their antiviral properties and to *in silico* studies to determine the interactions
2 with 3CL^{pro}. Compounds **14d**, **14n**, **14q**, **18f** and **18i** showed moderate activity against coronavirus 229E. A
3 molecular modeling work flow was developed based on previously reported 3CL^{pro} non-covalent inhibitors
4 and helped the identification of key molecular interactions. Application of this model to our library, supports
5 that the antiviral activity is mediated through the inhibition of 3CL^{pro}. Additional studies on the structure-
6 activity relationship will enable us to prepare new fused 1,2,3-triazole derivatives with enhanced antiviral
7 properties.

9 Acknowledgments

10 This work was supported by Katholieke Universiteit Leuven (KU Leuven), grants C32/15/033 and
11 ISPLA2/15/03. In addition, the authors gratefully acknowledge financial support from the Secretaria de Ciencia
12 y Técnica of the Universidad Nacional de Córdoba (SECYT-UNC), the Consejo Nacional de Investigaciones
13 Científicas y Técnicas (CONICET), and the Agencia Nacional de Promoción Científica y Técnica (ANPCyT).
14 The authors would also like to thank the GPGPU Computing Group from the Facultad de Matemática,
15 Astronomía y Física (FAMAF), Universidad Nacional de Córdoba, Argentina, for providing access to
16 computing resources. The authors also gratefully acknowledge the support of NVIDIA Corporation with the
17 donation of the Titan Xp GPU used for this research. Mario A. Quevedo wishes to thank OpenEye Scientific
18 Software and their Free Academic Licensing program for providing him with licenses to use the corresponding
19 software packages.

20 References

- 21 1. Bradburne AF, Bynoe ML, Tyrrell DAJ. Effects of a "New" Human Respiratory Virus in Volunteers. *Brit*
22 *Med J.* 1967; 3; 767-769.
- 23 2. Drosten C, Günther S, Preiser W, Van der Werf S, Brodt HR, Becker S, Rabenau H, Panning M,
24 Kolesnikova L, Fouchier RAM, Berger A, Burguière AM, Cinatl J, Eickmann M, Escriou N, Grywna K,
25 Kramme S, Manuguerra JC, Müller S, Rickerts V, Stürmer M, Vieth S, Klenk HD, Osterhaus ADME,
26 Schmitz H, Doerr HW. Identification of a novel coronavirus in patients with severe acute respiratory
27 syndrome. *N Engl J Med.* 2003; 348: 1967-1976. DOI: <https://doi.org/10.1056/NEJMoa030747>.
- 28 3. Kuiken T, Fouchier RAM, Schutten M, Rimmelzwaan GF, Van Amerongen G, Van Riel D, Laman JD, De
29 Jong T., Van Doornum G, Lim W, Ling AE, Chan PKS, Tam JS, Zambon MC, Gopal R, Drosten C, Van
30 der Werf S, Escriou N, Manuguerra JC, Stöhr K, Peiris JSM, Osterhaus ADME. Newly discovered
31 coronavirus as the primary cause of severe acute respiratory syndrome. *Lancet.* 2003; 362; 263-270.
32 [https://doi.org/10.1016/S0140-6736\(03\)13967-0](https://doi.org/10.1016/S0140-6736(03)13967-0).
- 33 4. Communicable Disease Surveillance and response; WHO. SARS case fatality ratio, incubation period.
34 http://www.who.int/csr/sars/archive/2003_05_07a/en/. Published 7 May 2003.
- 35 5. Van Der Hoek L, Pyrc K, Jebbink MF, Vermeulen-Oost W, Berkhout RJM, Wolthers KC, Wertheim-van
36 Dillen PME, Kaandorp J, Spaargaren J, Berkhout B. Identification of a new human coronavirus. *Nat*
37 *Med.* 2004; 10: 368-373. <https://doi.org/10.1038/nm1024>.
- 38 6. Woo PCY, Lau SKP, Chu C, Chan K, Tsoi H, Huang Y, Wong BHL, Poon RWS, Cai JJ, Luk W, Poon
39 LLM, Wong SSY, Guan Y, Peiris JSM, Yuen K. Characterization and Complete Genome Sequence of a
40 Novel Coronavirus, Coronavirus HKU1, from Patients with Pneumonia. *J Virol.* 2005; 79: 884-895.
41 <https://doi.org/10.1128/JVI.79.2.884-895.2005>.

- 1 7. Zaki AM, Van Boheemen S, Bestebroer TM, Osterhaus ADME, Fouchier RAM. Isolation of a Novel
2 Coronavirus from a Man with Pneumonia in Saudi Arabia. *N Engl J Med*. 2012; 367: 1814-1820.
3 <https://doi.org/10.1056/NEJMoa1211721>.
- 4 8. Chan JFW, Lau SKP, To KKW, Cheng VCC, Woo PCY, Yuen KY. Middle East Respiratory syndrome
5 coronavirus: Another zoonotic betacoronavirus causing SARS-like disease. *Clin Microbiol Rev*. 2015;
6 28: 465-522. <https://doi.org/10.1128/CMR.00102-14>.
- 7 9. Zumla A, Chan JFW, Azhar EI, Hui DSC, Yuen KY. Coronaviruses-drug discovery and therapeutic
8 options. *Nat Rev Drug Discov*. 2016; 15: 327-347. <https://doi.org/10.1038/nrd.2015.37>.
- 9 10. Pillaiyar T, Manickam M, Namasivayam V, Hayashi Y, Jung SH. An overview of severe acute
10 respiratory syndrome-coronavirus (SARS-CoV) 3CL protease inhibitors: Peptidomimetics and small
11 molecule chemotherapy. *J Med Chem*. 2016; 59: 6595-6628.
12 <https://doi.org/10.1021/acs.jmedchem.5b01461>.
- 13 11. Anand K, Ziebuhr J, Wadhvani P, Mesters JR, Hilgenfeld R. Coronavirus Main Proteinase (3CL pro)
14 Structure: Basis for Design of Anti-SARS Drugs. *Science*. 2003; 300:
15 1763-1767. <https://doi.org/10.1126/science.1085658>.
- 16 12. Thomas J, Jana S, John J, Liekens S, Dehaen W. A general metal-free route towards the synthesis of
17 1,2,3-triazoles from readily available primary amines and ketones. *Chem Commun*. 2016; 52: 2885-
18 2888. <https://doi.org/10.1039/c5cc08347h>.
- 19 13. Yang S, Chen SJ, Hsu MF, Wu JD, Tseng CTK, Liu YF, Chen HC, Kuo CW, Wu CS, Chang LW, Chen
20 WC, Liao SY, Chang TY, Hung HH, Shr HL, Liu CY, Huang YA, Chang LY, Hsu JC, Peters CJ, Wang
21 AHJ, Hsu MC. Synthesis, crystal structure, structure-activity relationships, and antiviral activity of a
22 potent SARS coronavirus 3CL protease inhibitor. *J Med Chem*. 2006; 49: 4971-4980. <https://doi.org/10.1021/jm0603926>.
- 24 14. Chen LR, Wang YC, Lin YW, Chou SY, Chen SF, Liu LT, Wu YT, Kuo CJ, Chen TSS, Juang SH.
25 Synthesis and evaluation of isatin derivatives as effective SARS coronavirus 3CL protease inhibitors.
26 *Bioorg. Med Chem Lett*. 2005; 15: 3058-3062. <https://doi.org/10.1016/j.bmcl.2005.04.027>.
- 27 15. Wu CY, King KY, Kuo CJ, Fang JM, Wu YT, Ho MY, Liao CL, Shie JJ, Liang PH, Wong CH. Stable
28 Benzotriazole Esters as Mechanism-Based Inactivators of the Severe Acute Respiratory Syndrome 3CL
29 Protease. *Chem Biol*. 2006; 13: 261-268. <https://doi.org/10.1016/j.chembiol.2005.12.008>.
- 30 16. Ghosh AK, Gong G, Grum-Tokars V, Mulhearn DC, Baker SC, Coughlin M, Prabhakar BS, Sleeman K,
31 Johnson ME, Mesecar AD. Design, synthesis and antiviral efficacy of a series of potent chloropyridyl
32 ester-derived SARS-CoV 3CLpro inhibitors. *Bioorg Med Chem Lett*. 2008; 18: 5684-5688.
33 <https://doi.org/10.1016/j.bmcl.2008.08.082>.
- 34 17. Zhang J, Huitema C, Niu C, Yin J, James MNG, Eltis LD, Vederas JC. Aryl methylene ketones and
35 fluorinated methylene ketones as reversible inhibitors for severe acute respiratory syndrome (SARS)
36 3CLike proteinase. *Bioorg Chem*. 2008; 36: 229-240. <https://doi.org/10.1016/j.bioorg.2008.01.001>.
- 37 18. Jacobs J, Grum-Tokars V, Zhou Y, Turlington M, Saldanha SA, Chase P, Egger A, Dawson ES,
38 BaezSantos YM, Tomar S, Mielech AM, Baker SC, Lindsley CW, Hodder P, Mesecar A, Stauffer SR.
39 Discovery, synthesis, and structure-based optimization of a series of N -(tert -Butyl)-2-(N -arylamido)-
40 2(pyridin-3-yl) acetamides (ML188) as potent noncovalent small molecule inhibitors of the severe acute
41 respiratory syndrome coronavirus (SARS-CoV) 3CL. *J Med Chem*. 2013; 56: 534-546.
42 <https://doi.org/10.1021/jm301580n>.
- 43 19. Turlington M, Chun A, Tomar S, Egger A, Grum-Tokars V, Jacobs J, Daniels JS, Dawson E, Saldanha
44 A, Chase P, Baez-Santos YM, Lindsley CW, Hodder P, Mesecar AD, Stauffer SR. Discovery of
45 N(benzo[1,2,3]triazol-1-yl)-N-(benzyl)acetamido)phenyl) carboxamides as severe acute respiratory
46 syndrome coronavirus (SARS-CoV) 3CLpro inhibitors: Identification of ML300 and noncovalent
47 nanomolar inhibitors with an induced-fit binding. *Bioorg Med Chem Lett*. 2013; 23: 6172-6177.
48 <http://doi.org/10.1016/j.bmcl.2013.08.112>.

- 1 20. Gallagher MJ, Mann FG. The structure and properties of certain polycyclic indolo- and
2 quinolinoderivatives. Part XV. Derivatives of 1-phenyl-4-piperidone and its phosphorus and arsenic
3 analogues. *J Chem Soc.* 1962; 23: 5110.
- 4 21. Schön U, Messinger J, Buckendahl M, Prabhu MS, Konda A. An improved synthesis of N-aryl and
5 Nheteroaryl substituted piperidones. *Tetrahedron Lett.* 2007; 48: 2519-2525.
6 <http://doi.org/10.1016/j.tetlet.2007.02.053>.

ACCEPTED MANUSCRIPT